JACS
JOURNAL OF THE AMERICAN CHEMICAL SOCIETY
Article
pubs.acs.org/JACS

Establishing the Ground State of the Disjoint Diradical Tetramethyleneethane with Quantum Monte Carlo

Zachary D. Pozun, Xiaoge Su, and Kenneth D. Jordan*

Department of Chemistry, University of Pittsburgh, Pittsburgh, Pennsylvania 15260, United States

Supporting Information

ABSTRACT: The nature of the electronic ground state of the tetramethyleneethane (TME) diradical has proven to be a challenge for both experiment and theory. Through the use of quantum Monte Carlo (QMC) methods and multireference perturbation theory, we demonstrate that the lowest singlet state of TME is energetically lower than the lowest triplet state at all values of the torsional angle between the allyl subunits. Moreover, we find that the maximum in the potential energy curve for the singlet state occurs at a torsional angle near 45°, in contrast to previous calculations that placed the planar structure of the singlet state as the highest in energy. We also show that the CASPT2 method when used with a sufficiently large reference space and a sufficiently flexible basis set gives potential energy curves very close to those from the QMC calculations. Our calculations have converged the singlet−triplet gap of TME as a function of methodology and basis set. These results provide insight into the level of theory required to properly model diradicals, in particular disjoint diradicals, and provide guidelines for future studies on more complicated diradical systems.

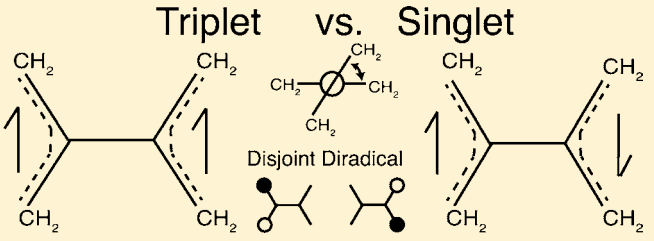

INTRODUCTION

The tetramethyleneethane (TME) molecule is a disjoint, non-Kekulé diradical that, since its synthesis by Dowd,[1] has remained a challenge for both experimental and theoretical analysis. Diradical character, which arises when two electrons occupy two degenerate molecular orbitals, is an important electronic structure phenomenon. Among the systems and processes where diradical character plays an important role are silicon surface reconstruction,[2] surface-mediated cycloaddition reactions,[3,4] self-assembly of rotaxanes on titania nanoparticles,[5] and reactions in cometary ices.[6] TME, as the simplest disjoint diradical, is an important model system that provides key insight into the behavior of more complicated diradical systems.

TME consists of two allyl fragments bonded at the central carbons. It thus has six π orbitals that contain six electrons. The four methylene CH_2 groups are equivalent by symmetry, as are the two central carbon atoms. As a non-Kekulé molecule, TME cannot be represented by a valence bond structure where the electrons are delocalized into a network of conjugated double bonds. Possible TME resonance structures are shown in Figure 1a.

The two frontier orbitals of TME are nearly degenerate and contain two electrons.[7,8] The disjoint nature of these orbitals is most readily seen in a localized orbital representation, as illustrated in Figure 1b. Each of the localized orbitals is nonbonding and is localized on one of the allyl subunits. Because of the small interaction between the two disjoint orbitals, the lowest energy singlet and triplet states are expected to lie very close in energy. The low-lying triplet state is expected to be reasonably well-described by a single Slater determinant, while the singlet state requires, at a minimum, two Slater determinants for its description.[7,9]

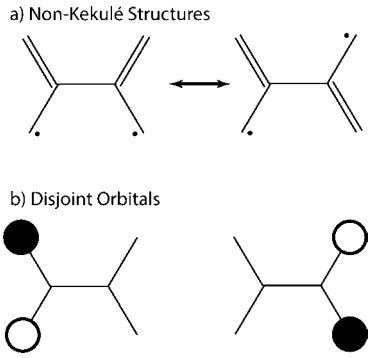

Figure 1. (a) Two possible resonance structures of TME. (b) Localized nonbonding frontier orbitals.

TME originally attracted interest due to the possibility that it could be used as an organic magnet if the ground electronic state were a triplet.[10] It has been suggested as a building block for electrically conductive polymers[11,12] and has also been used to generate organoruthenium complexes with unique dianionic character.[13] Its derivatives have been used as photoinduced electron transfer centers to promote rearrangements in cyclic ketones.[14] TME frequently is used to model the spin states of more complicated disjoint diradicals.[8,15,16] Thus, establishing the level of theory needed to properly characterize the

Received: June 14, 2013
Published: August 16, 2013

   dx.doi.org/10.1021/ja406002n | J. Am. Chem. Soc. 2013, 135, 13862−13869

electronic states of TME has implications for modeling a large class of molecules.

One of the major challenges in determining the relative stability of the lowest energy singlet and triplet states of TME is that the molecule can rotate about the central C−C bond while maintaining D_2 symmetry as shown in Figure 2. This extra

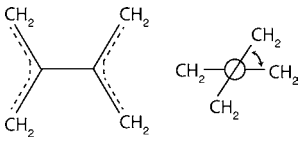

Figure 2. The TME molecule and the central torsional angle between the allylic subunits.

degree of freedom in the structure raises the possibility that the singlet and triplet potential energy curves could cross one another as the torsional angle is varied. Thus, determining the ordering of these two low-lying states is a difficult theoretical and experimental challenge.

On the basis of simple molecular orbital (MO) considerations, Longuet-Higgins[17] concluded that TME has a triplet ground state. When Dowd first synthesized TME, he found that it gave rise to an electron paramagnetic resonance (EPR) spectrum that indicates a sizable population of the triplet state under experimental conditions.[1] Subsequent experimental work designed to stabilize the molecule in a matrix also concluded that the triplet was lower in energy with a torsional angle of approximately 45°.[15,18] On the other hand, photoelectron spectroscopy of the TME^- ion provides strong evidence that the ground state of TME is the singlet state at the 90° torsional angle.[19] EPR experiments on TME derivatives are also consistent with these having singlet ground states.[20,21]

The results of different quantum chemistry calculations on TME are also contradictory. Calculations using a two-configurational self-consistent field treatment of the singlet state and a single configuration for the triplet state predicted that the singlet and triplet potential curves cross as a function of the torsional angle.[22] However, when the calculations were extended to configuration interaction with single and double excitations (CISD) in the valence space, it was found that the singlet was lower in energy for all values of the torsional angle.[22] In contrast, CISD calculations allowing excitations into the entire virtual space and again using two references for the singlet concluded that the triplet state minimum is lower in energy than the singlet state minimum.[23]

A complete active space self-consistent field (CASSCF) calculation with the six π electrons distributed all possible ways in an active space comprised of the six π orbitals similarly determined the energy difference between the minima on the singlet and triplet state potential energy curves favored the singlet state.[24] A difference dedicated configuration interaction (DDCI) calculation predicted near-degeneracy of the singlet and triplet states at torsional angles in the range of 40−50°;[25] a similar result was obtained by spin-restricted ensemble-referenced Kohn−Sham (REKS)[26] calculations.

In contrast, multireference coupled cluster calculations (MRCC) using two reference configurations for the singlet state and a single reference for the triplet state predicted that the singlet state is lower in energy than the triplet state;[27] however, inclusion of triple excitations in the MRCC calculations increased the magnitude of the gap by a factor of 2.[28] Interestingly, the minimum energy structure of the singlet state occurred at a twist angle of 30° with the inclusion of triple excitations and at 90° without triplet excitations. Recently, Chattopadhyay et al. reported improved virtual orbital complete active space configuration interaction (IVO-CASCI) calculations that placed the singlet below the triplet at all torsional angles and gave the 90° twisted structure as the minimum of the singlet state.[29]

The history of experimental and theoretical studies of TME clearly indicates that the magnitude of the singlet−triplet gap and the shape of the singlet twisting potential are not well established. To determine the energies of the lowest singlet and triplet states of TME as a function of torsional angle and to reconcile the various experimental and theoretical results, we apply quantum Monte Carlo (QMC) techniques to this system.

QMC methods explicitly account for electron correlation effects by numerically integrating the Schrödinger equation. An antisymmetrized trial wave function is generated from density functional theory (DFT), Hartree−Fock (HF), or CASSCF calculations and then multiplied by a Jastrow factor, which accounts for short-range electron−electron and electron−nuclear interactions.[30] The parameters in the trial function are optimized using the variational Monte Carlo (VMC) method.[31−33] Although the VMC method can recover much of the correlation energy at minimal computational cost, it is not sufficiently accurate for resolving small energy differences.[34] As a result, VMC calculations are generally followed by diffusion Monte Carlo (DMC) calculations.[35] In contrast to VMC, the DMC method, in principle, is able to solve the Schödinger equation exactly by stochastic integration. In practice, however, the fermion sign problem prevents an exact solution.[32] The usual strategy of dealing with the fermion sign problem is to fix the nodes in the trial wave function in the DMC procedure, a result of which is that the resulting DMC energy has a small error due to the fixed nodes.[36−38]

Despite the status of TME as the simplest disjoint diradical and as a model system for more complicated disjoint diradicals, the relative energies of its lowest singlet and triplet states as a function of the dihedral angle between the allylic subunits is clearly still an open question. In the present study, we apply QMC methods to TME and show that many of the earlier theoretical treatments suffered from an unbalanced treatment of electron correlation effects in the two low-lying electronic states as well as from limitations in the atomic basis sets that were employed.

■ COMPUTATIONAL METHODS

In the present study, the twisting potential energy curves of the singlet state were first calculated using restricted Hartree−Fock (RHF),[39] Møller−Plesset second-order perturbation theory (MP2),[40] and coupled cluster singles and doubles with perturbative triples (CCSD(T)).[41,42] None of these calculations is expected to provide a good description of the singlet state on account of the static correlation arising from the near degeneracy of the frontier orbitals. We include these calculations to illustrate the importance of static as compared to dynamical correlation effects. The potential energy curves of the triplet state were calculated using restricted open-shell Hartree−Fock (ROHF) and MP2 and CCSD(T) methods based on this reference.[43−45] We also compare the singlet and triplet energies as calculated with Kohn−Sham DFT[46] using the Perdew−Burke−Ernzerhof hybrid functional.[47,48] All of these calculations made use of the cc-pVTZ[49] basis set and were performed with the Gaussian 09 program.[50]

In addition, we have optimized the geometries of the two states as a function of torsional angle using the CASSCF(6,6) method with analytical gradients[51−53] and the cc-pVTZ basis set. As in previous

dx.doi.org/10.1021/ja406002n | J. Am. Chem. Soc. 2013, 135, 13862−13869

work, CAS(6,6) denotes a CASSCF calculation with the six π electrons distributed over the six π orbitals. QMC calculations were carried out using the CAS(6,6) optimized geometries and using trial functions that retained the most important determinants in the CASSCF expansions such that the sum of the squares of the coefficients of the retained configurations was 0.995. The trial functions for the QMC calculations were represented in terms of the cc-pV5Z(sp)+2d-CDF[54] basis set and utilized the Trail–Needs norm-conserving Dirac–Fock pseudopotentials.[55,56] QMC calculations were performed using the CASINO package.[57]

The form of the Jastrow factors given by Drummond et al. was employed for all QMC calculations.[58] The electron–electron (u) and the electron–nucleus terms (χ) were expanded to eighth order in interparticle distance. The electron–electron–nucleus term (f) was expanded to second order in interparticle distances. To prevent spin contamination, extra constraints were imposed for the singlet state trial function. Specifically, the parameters in the u and f terms were constrained such that the terms for two coalescing spin-up electrons were the same as for two spin-down electrons. The χ term was similarly constrained such that the terms for a spin-up electron were the same as a spin-down. The Jastrow factors in VMC calculations were optimized for both spin states for each torsional angle considered. The coefficients in the multideterminant expansions were also optimized. The coefficients for spin-flipped pairs of determinants in the expansion for the singlet state were constrained during optimization to remain equal so that spin contamination was avoided. The energy minimization method was employed for VMC optimization.[59]

During the VMC calculations, 50 000 walkers were propagated for 1 000 000 steps. During the DMC[60] calculations, 40 000 walkers were propagated for 100 000 Monte Carlo steps. The t-move scheme of Casula[61] was used to treat the nonlocal portion of the pseudopotentials. DMC calculations were performed at time steps of 0.005, 0.0075, and 0.01 au, and the energies at these time steps were linearly extrapolated to the t = 0 limit. The DMC energies and statistical errors were extracted using reblocking.[62]

For comparison to the QMC results, we carried out complete active space second-order perturbation theory (CASPT2)[63,64] calculations as implemented in the MOLPRO package.[65,66] The CASPT2 calculations were carried out using both CAS(2,2) and CAS(6,6) reference spaces and each of the cc-pVDZ, cc-pVTZ, and cc-pVQZ basis sets.[49]

RESULTS

By definition, the electron correlation energy within a given basis set is the difference between the HF and full configuration interaction (CI) energies in that basis set. The correlation energy is commonly broken into static and dynamical contributions.[67] Static correlation derives from near degeneracy effects, while dynamical correlation is the remaining portion of the correlation energy. Within the context of the DMC method, the amount of correlation energy that can be recovered is limited by the quality of the nodal surface in the fixed-node approximation. In general, in systems where static correlation effects are important, a trial function with more than one configuration is necessary to generate a suitable nodal surface.[68] In the following sections, we analyze the role of static and dynamical correlation in determining the potential energy curves for the singlet and triplet states of TME.

The Role of Static Correlation in TME. When the dihedral angle between the allylic subunits is 0°, the TME molecule is planar and belongs to the D_{2h} point group. At a dihedral angle of 90°, the molecule has D_{2d} symmetry. At intermediate angles, the molecule has D_2 symmetry. These three cases are shown in Figure 3. Each of the six carbon atoms in TME is sp^2 hybridized, and, as noted previously, there are six π electrons.

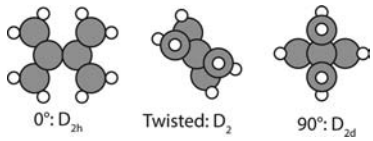

Figure 3. The TME molecule at different torsional angles.

The π orbitals from an ROHF calculation on the triplet state of the planar molecule are shown in Figure 4. In the simplest

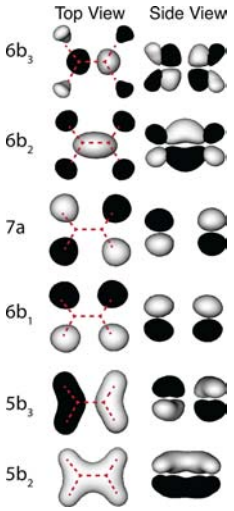

Figure 4. π orbitals of TME from ROHF calculations on the $^3B_1$ state of the planar structure. The red dotted line indicates the carbon skeleton of the molecule.

wave functions for the singlet and triplet states, the $5b_2$ and $5b_3$ orbitals are doubly occupied. The next two π orbitals, the $6b_1$ and 7a frontier orbitals, are nearly degenerate, and in the triplet state each is singly occupied. At a minimum, the wave function for the singlet state should include the $|...(5b_2)^2(5b_3)^2(6b_1^2)\rangle$ and $|...(5b_2)^2(5b_3)^2(7a)^2\rangle$ configurations. The $6b_2$ and $6b_3$ π orbitals are not occupied in the simplest wave function for either state.

As shown in Figure 5, the $6b_1$ and 7a orbitals cross near 40°. Figure 6 reports the singlet and triplet twisting potentials of TME obtained at the HF, MP2, CCSD(T), and PBE0 levels of theory. The barriers in the singlet potentials shown are due to

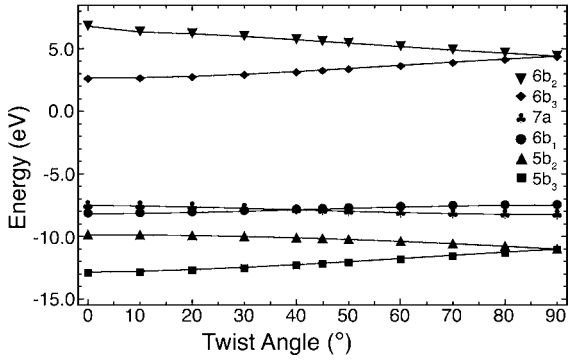

Figure 5. The orbital energies of TME as a function of the torsional angle between the allyl subunits. The orbital energies are calculated for the triplet state using the cc-pVTZ basis set and the ROHF procedure as implemented in MOLPRO.

dx.doi.org/10.1021/ja406002n | J. Am. Chem. Soc. 2013, 135, 13862–13869

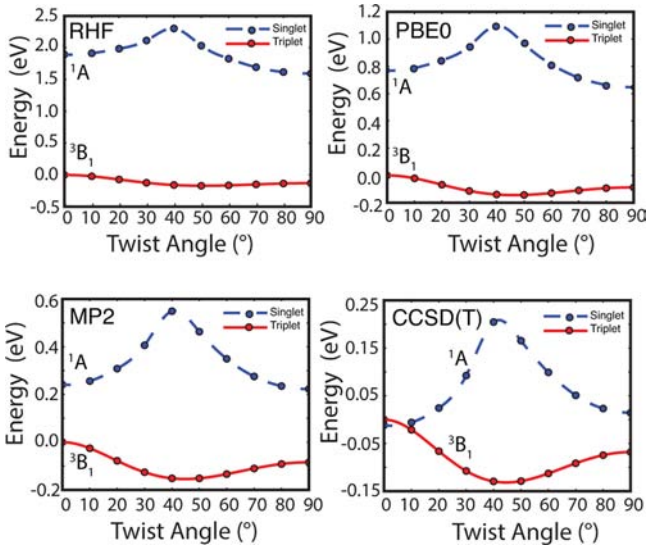

Figure 6. The singlet−triplet gap of TME as a function of torsional angle for the HF, PBE0, MP2, and CCSD(T) methods in the cc-pVTZ basis. In each method, the ground state is predicted to be a triplet state with the singlet lying higher in energy. The energy of the $^3B_1$ state at the torsional angle of 0° is taken as the zero of energy.

the change of the HF or Kohn−Sham wave functions from $|...(5b_2)^2(5b_3)^2(6b_1^2)\rangle$ to $|...(5b_2)^2(5b_3)^2(7a)^2\rangle$ as a result of the orbital crossing. At the HF level, the singlet is calculated to lie nearly 2.5 eV higher in energy than the triplet state. The singlet−triplet gap decreases when correlation effects are included and falls to approximately 0.35 eV at the CCSD(T) level for a torsional angle near 40°. However, even the CCSD(T) method does not properly describe the static correlation that arises from the near degeneracy of the frontier orbitals in the singlet state.

As noted above, to describe static correlation effects in the singlet state, one must adopt, at a minimum, a CAS(2,2) active space. However, as seen from Figure 7, which compares the

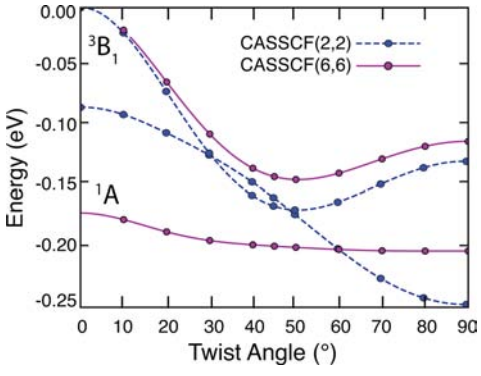

Figure 7. The CASSCF(2,2) and CASSCF(6,6) twisting curves of TME calculated using the cc-pVQZ basis set. The energy of the $^3B_1$ state at 0° is taken as the zero of energy.

twisting potentials of the singlet and the triplet states calculated with CAS(2,2) and CAS(6,6) reference spaces, the shape of the singlet potential undergoes a qualitative change in going from the CAS(2,2) to the CAS(6,6) space. In particular, the singlet twisting potential is much flatter when evaluated at the CAS(6,6) level. This effect is primarily a consequence of the relatively small energy separation between the $5b_3$ orbital and the two frontier orbitals. Hence, the CAS(2,2) space is inadequate for describing static correlation effects in the singlet state. For this reason, we use the CAS(6,6) trial functions, modified as detailed below, for the QMC calculations.

The Role of Dynamical Correlation in TME. As previously mentioned, the QMC calculations were carried out retaining the most important determinants in the CAS(6,6) expansion with a cutoff criterion such that the sum of determinant coefficients squared is 0.995. As the molecule is twisted toward 90°, more determinants are required to meet the cutoff criterion due to the decreasing energy gap between the $5b_2$ orbital and the frontier orbitals. At the 90° torsional angle, 38 determinants are retained in the singlet state and 23 in the triplet state. Care was taken to not break symmetry by the truncation.

Table 1 summarizes the results of the VMC calculations on TME at a torsional angle of 40°. Results are reported without a

Table 1. Role of the Jastrow Factor in the VMC Calculations for the Singlet State of TME at a Dihedral Angle of 40° and Employing a Truncated CAS(6,6) Trial Function with the cc-pV5Z(sp)+2d-CDF Basis Set[a]

trial function	energy (eV)	variance (eV)	S−T gap (eV)
no Jastrow	−1023.72	180.1	−0.517
e−e and e−n	−1048.88	19.864	−0.313
e−e−n added	−1050.05	18.639	−0.250
coeff opt.	−1050.68	18.258	0.088

[a]The calculations with Jastrow factors used energy minimization. The energies in the first three rows were obtained without optimization of the CI coefficients. With added terms, all coefficients were reoptimized.

Jastrow factor as well as with various terms included in the Jastrow factor. Although the CAS(6,6) calculations employing the full CI expansion place the singlet state lower in energy than the triplet state, with the truncated space the triplet state is lower in energy. However, the effect of truncation is negligible for the calculations at the DMC level. In addition, there is a sizable drop in both the energy and the variance upon inclusion of the e−e and e−n Jastrow factors, while the inclusion of the e−e−n term leads to a much smaller drop in energy and variance. When the CI coefficients are optimized along with the variables in the Jastrow factor, the VMC energy is further lowered, and the sign of the singlet−triplet gap changes. Importantly, the singlet state is stabilized relative to the triplet by both the introduction of the Jastrow factor and upon CI coefficient optimization in the VMC step.

The VMC energies of TME as a function of torsional angle obtained using multideterminant trial functions combined with three-term Jastrow factors are reported in Figure 8. At both 0° and 90°, the singlet−triplet ordering is resolved outside of the error bars on the energies. At these angles, the singlet−triplet splittings are approximately the same as predicted by the CASSCF(6,6) calculations. At intermediate angles, however, the single and triplet VMC energies overlap after taking into account the large statistical error bars in the calculations. The singlet state is higher in energy at dihedral angles near 45° than at 0° and 90°.

Table 2 reports the energy of the singlet state and the singlet−triplet gap for three sets of DMC calculations. When using a single determinant as a trial function for both the singlet and the triplet states, the triplet is calculated to be 1.26 eV more

dx.doi.org/10.1021/ja406002n | J. Am. Chem. Soc. 2013, 135, 13862−13869

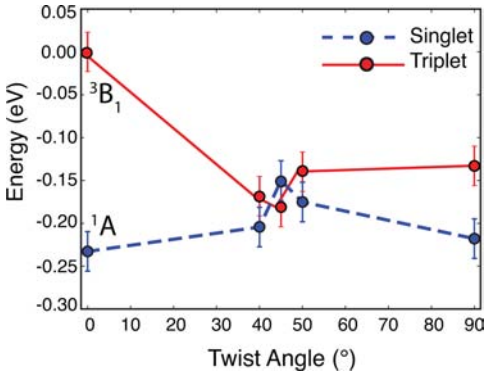

Figure 8. Plot of the VMC energies as a function of torsional angle. The zero of energy is that of the triplet state at 0°. At each angle and spin state, the coefficients in the Jastrow factor and truncated CAS(6,6) trial function are optimized. The trial functions are expressed in the cc-pV5Z(sp)+2d-CDF basis.

Table 2. DMC Energies (τ = 0.005 au) for the Singlet State and Singlet−Triplet Gaps of TME at Torsional Angle of 40°[a]

trial function	energy (eV)	S−T gap (eV)
HF	−1051.247(5)	−1.264(3)
CAS(2,2)	−1052.504(1)	−0.004(1)
truncated CAS(6,6)	−1052.857(5)	0.042(6)

[a]The coefficients in the truncated CAS(6,6) trial functions and the Jastrow factors have been optimized for each calculation. The cc-pV5Z(sp)+2d-CDF basis set was employed for all calculations.

stable than the singlet state. This outcome demonstrates the inadequacy of the nodal surface of the singlet state as described by a single Slater determinant. In fact, both the MP2 and the CCSD(T) methods yield smaller singlet−triplet gaps than the DMC method when using a trial function with a single determinant trial function. Interestingly, the singlet−triplet gap from the DMC calculations with single determinant trial functions is nearly the same as that obtained from the DFT calculations, which are known to be inadequate for describing static correlation effects.[69]

Table 2 also reports the DMC energies of the singlet state and the singlet−triplet gap obtained using trial functions generated from the truncated CAS(6,6) spaces. Unlike wave function methods based on a CI expansion that adds explicit correlation to the HF wave function, adding more determinants to the trial wave function for DMC calculations systematically improves the nodal surface.[68] DMC, under the fixed node approximation, recovers all of the correlation energy within a given nodal surface. By adding more determinants to the trial wave function and optimizing their coefficients, a larger percentage of correlation energy can be recovered. As Table 2 shows, adding more determinants converges both the energy and the singlet−triplet gap. Thus, the magnitude of the fixed node error is minimized, and the energies are converged as a function of number of determinants included in the expansion.

The twisting potentials at the DMC level using the multireference trial functions for the singlet and triplet states are shown in Figure 9. The potentials of both the singlet and the triplet states obtained from the DMC calculations differ somewhat from the CAS(6,6) calculations. The most significant difference is that the twisting potential of the singlet state is significantly flatter in the DMC than in the CAS(6,6)

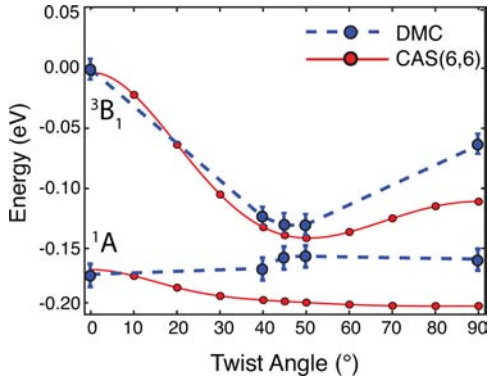

Figure 9. Torsional potential energy curves for the singlet and triplet states of TME obtained from DMC calculations with a multideterminant trial function as well as from CAS(6,6) calculations with the cc-pV5Z(sp)+2d-CDF basis set. DMC energies are calculated at a time step of τ = 0.005 au. The trial functions for the DMC calculations were taken from a truncation of the CAS(6,6) expansion. The zero of energy is the triplet state at 0° for each method.

calculations, in which the singlet potential has a maximum in the range of 40°−50°.

As noted previously, the DMC calculations were carried out at finite time steps, which introduces errors in the energies. However, as seen in Figure 10, over the whole range of

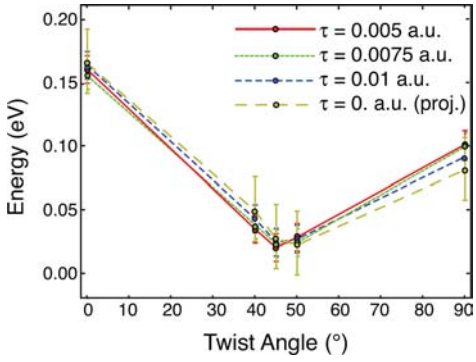

Figure 10. The singlet−triplet gap of TME as a function of torsional angle for DMC calculations at three different time steps and linearly extrapolated to the τ = 0 limit. The gaps calculated at the various time steps agree to within the error bars. At each angle and spin state, the coefficients in the Jastrow factor and truncated CAS(6,6) trial function are optimized. The trial functions are expressed in the cc-pV5Z-(sp)+2d-CDF basis.

torsional angles, the singlet−triplet gap is essentially independent of the time step. Although energies are obtained by linearly extrapolating the energies at the three time steps to the τ = 0 limit, it is sufficient to use a single time step at each torsional angle.

The DMC results presented above motivated us to carry out CASPT2 calculations of the singlet and triplet twisting potentials using both CAS(2,2) and CAS(6,6) reference spaces and employing three different basis sets. CASPT2 is significantly less computationally demanding than DMC; however, it is more much more sensitive to the basis set and active space employed. As seen from Figure 11, the CAS(6,6)PT2 twisting potentials calculated using the cc-pVTZ and cc-pVQZ basis sets are quite similar in shape to the corresponding DMC potentials reported above. However, for the singlet state, the CAS(6,6)PT2 potential obtained with

dx.doi.org/10.1021/ja406002n | J. Am. Chem. Soc. 2013, 135, 13862−13869

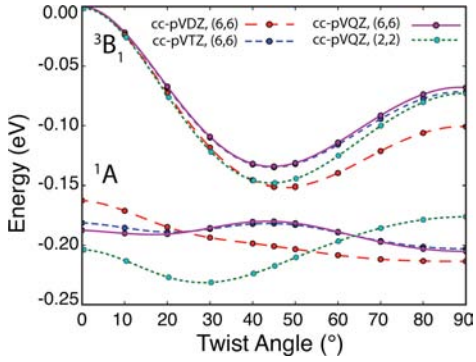

Figure 11. The singlet and triplet curves of TME as calculated by the CASPT2 method for different basis sets.

the cc-pVDZ basis set is qualitatively different from those obtained with the two larger basis sets.

To determine whether the sensitivity to the basis set is due to the high angular momentum functions, we also carried out CAS(6,6)PT2 calculations with the cc-pVTZ′ basis set, which omits from the standard cc-pVTZ basis set the f functions on the C atoms and the d functions on the H atoms. The twisting potential for the singlet state obtained with the cc-pVTZ′ basis set is similar in shape to that obtained using the cc-pVDZ basis set. CAS(6,6)PT2 calculations were also performed with the cc-pVTZ basis set modified by omitting only the d functions on the H atoms while retaining the f functions on the C atoms. This basis set resulted in a twisting potential for the singlet state that is nearly identical to that obtained using the full cc-pVTZ basis set; this result establishes that the inclusion of the f basis functions on the C atoms is essential for accurately describing the singlet state twisting potential of TME with traditional wave function methods.

It is also seen from Figure 11 that the CAS(2,2)PT2 procedure gives a twisting potential for the singlet state that is qualitatively different from that obtained using the CAS(6,6)-PT2 procedure. This effect is a consequence of the importance in the CAS(6,6) wave function of configurations involving excitations out of the $5b_2$ and $5b_3$ orbitals. Thus, a two-configurational reference is insufficient for CASPT2 calculations on the singlet state of TME. In contrast, the CAS(6,6)PT2 method, when used with either a cc-pVTZ or a cc-pVQZ basis set, gives singlet and triplet potentials that are in close agreement with the DMC results.

Under conditions where the $(\hat{H}^{(0)}-E^{(0)})$ term in the perturbative expansion becomes singular, the CASPT2 wave function does not converge. In these cases, level shift methods are required to remove the singularity.[70] Although we do not observe this problem, we have tested level shifts of 0.05, 0.1, 0.2, and 0.3 au and found a negligible effect on the singlet−triplet gap of the converged CAS(6,6)PT2/cc-pVQZ calculations.

Pittner et al.[27] and Bhaskaran-Nair et al.[28] carried out two-reference MRCC calculations on the lowest-lying singlet state of TME. When including only single and double excitations in the MRCC expansion (MRCCSD), the maximum in the singlet state twisting potential of TME occurred at a dihedral angle of 0°.[27] Two-reference MRCC calculations with iterative triples (MRCCSD(T)) give a shallow minimum in the potential energy curve of the singlet state at a dihedral angle of 30°.[28] However, these calculations used the cc-pVTZ′ basis set that excludes f functions on the carbon atom. We have demonstrated that the inclusion of the carbon f functions and using a reference space with more than two configurations are both important for properly characterizing the singlet state of TME. Table 3 summarizes the results for TME obtained from various CASPT2 and MRCC calculations as well as from the DMC calculations of the present study.

Table 3. Minima and Maxima of the Torsional Potential of the Singlet State of TME As Calculated with Different Methods

method	basis set	minima	maxima
CAS(2,2)PT2	cc-pVQZ	30°	0° and 90°
CAS(6,6)PT2	cc-pVDZ	90°	0°
CAS(6,6)PT2	cc-pVQZ	0° and 90°	45°
MRCCSD[27]	cc-pVTZ′[a]	90°	0°
MRCCSD(T)[28]	cc-pVTZ′[a]	30°	0° and 90°
CAS(6,6)PT2	cc-pVTZ′[a]	90°	0°
DMC	cc-pV5Z(sp)+2d-CDF	0° and 90°[b]	40°−50°

[a]No d functions on H atoms and no f functions on C atoms. [b]Energies at twist angles of 0° and 90° agree within statistical error.

DISCUSSION

Our DMC and CASPT2 calculations on TME indicate that electron correlation effects beyond those recovered at the CAS(6,6) level are more important for the singlet state at the torsional angle of 0° than at 45°. Interestingly, the REKS approach,[26] which accounts for static correlation in a CAS-like manner and dynamical correlation in a DFT-like manner, gives for the singlet state a twisting potential of qualitatively the same shape as those obtained by VMC, DMC, and CAS(6,6)PT2 calculations.

Our CAS(6,6)PT2 calculations demonstrate that a basis set at least as large as cc-pVTZ is required to properly describe the shape of the twisting potential of the singlet state of TME when using wave function-based methods. Although Pittner et al.[27] and Bhaskaran-Nair et al.[28] used two-reference coupled cluster methods to describe correlation effects, the basis set used in their studies did not contain f functions on the C atoms. Both the omission of the f functions and the restriction of the reference space to two configurations leads to errors in the shape of the calculated potential for the singlet state of TME.

Bhaskaran-Nair et al. reported singlet−triplet gaps for TME that range from −0.14 to 0.67 eV, depending upon the approximations used in the coupled-cluster expansion. This range of results illustrates the challenge of balancing the correlation effects in the singlet and triplet states of TME when using such methods. The DMC method is more successful in providing a balanced treatment of the electron correlation effects in the two states. As long as the trial function employed provides a suitable description of the nodal surface, the DMC method essentially recovers all of the electron correlation in the problem. Thus, the problems introduced by truncating the configuration space are avoided. Moreover, the energies obtained by DMC calculations are relatively insensitive to the choice of the basis set used to represent the trial function than are traditional wave function approaches.

As related to previous experimental work, our DMC calculations indicate that TME in the singlet state has a very small barrier to rotation about the central C−C bond and that, at intermediate twist angles, the vertical singlet−triplet gap is only about 0.02 eV. This small gap is consistent with EPR

dx.doi.org/10.1021/ja406002n | J. Am. Chem. Soc. 2013, 135, 13862−13869

spectra[1] that detected the triplet state of TME. The singlet is not EPR active, so the weak triplet signal was originally interpreted as evidence of a triplet ground state.

Negative ion photoelectron spectroscopy measurements provided evidence that the singlet is lower in energy than the triplet. The ground state of the anion of TME is a $^2B_1$ state with its potential energy minimum at a torsional angle of 90°. Two low-lying electronic states of neutral TME were observed in the photoelectron spectrum. These states were assigned as the $^3B_1$ and ^1A states with the ^1A state lying lower in energy. The singlet−triplet gap was measured to be 0.13 ± 0.013 eV between the $^3B_1$ and ^1A states at the 90° torsional angle. This result is in good agreement with our DMC (τ = 0.005 au) singlet−triplet gap of 0.10 ± 0.014 eV and our CASPT2 calculated singlet−triplet gap of 0.13 eV at a torsional angle of 90°.

Clifford et al.[19] estimated that, due to poor Franck−Condon overlap between the anion with the 90° torsional angle and the neutral triplet with the 45° torsional angle, the observed 0.13 eV gap is overestimated by approximately 0.04 eV. Our DMC and CASPT2 calculations, however, put the barrier to rotation for the triplet state at 0.07 eV, which suggests that the true singlet−triplet gap based on the energies of the two minima could be as small as 0.06 eV. Our calculations predict the separation between the minimum on the singlet potential and the minimum on the triplet potential to be 0.07 eV from CASPT2 and 0.04 eV from DMC. These results are consistent with the experimentally measured gap when corrected with the calculated barrier height of the triplet potential.

CONCLUSIONS

We have used the quantum Monte Carlo and CASPT2 approaches to calculate the torsional potentials of the lowest singlet and triplet states of TME. Multideterminant trial function were used to perform the DMC calculations, which give a torsional potential energy curve for the singlet state that is qualitatively different from that obtained in prior studies using traditional wave function methods. The CASPT2 method when performed with a sufficiently large active space and a sufficiently flexible basis set gives singlet and triplet potential energy curves with shapes and energy separations similar to those obtained from the DMC calculations. Our results conclusively demonstrate that the ground state of TME is a singlet and that the maximum in the torsional potential of the singlet state occurs at an angle of 45°, which is where the triplet state has its minimum.

The small singlet−triplet gap calculated at intermediate twist angles suggests the original EPR results were due to weak thermal population of the triplet state. Our results also are consistent with the results of negative ion photoelectron spectroscopy that measured the singlet−triplet gap at the 90° torsional angle. We also have demonstrated that previous theoretical studies were performed with insufficiently flexible atomic basis sets and, in most cases, also an inadequate treatment of static correlation effects in the singlet state. In addition, our calculations validate the use of CASPT2 for disjoint diradicals when used with flexible basis sets and a large active space.

ASSOCIATED CONTENT

Supporting Information

Coordinates for all optimized geometries and their absolute energies. This material is available free of charge via the Internet at http://pubs.acs.org.

AUTHOR INFORMATION

Corresponding Author

jordan@pitt.edu

Notes

The authors declare no competing financial interest.

ACKNOWLEDGMENTS

We wish to acknowledge Akila Gothandaraman and Albert DeFusco of the Center for Simulation and Modeling (SaM) at the University of Pittsburgh for assistance with calculations. We thank Michael Deible for many helpful discussions. Z.D.P. acknowledges support through NSF grant no. OCI-1225384. K.D.J. acknowledges support through NSF grant no. CHE-1111235.

REFERENCES

(1) Dowd, P. *J. Am. Chem. Soc.* **1970**, *92*, 1066−1068.
(2) Shoemaker, J.; Burggraf, L. W.; Gordon, M. S. *J. Chem. Phys.* **2000**, *112*, 2994−3005.
(3) Lu, X.; Wang, X.; Yuan, Q.; Zhang, Q. *J. Am. Chem. Soc.* **2003**, *125*, 7923−7929.
(4) Lu, X. *J. Am. Chem. Soc.* **2003**, *125*, 6384−6385.
(5) Long, B.; Nikitin, K.; Fitzmaurice, D. *J. Am. Chem. Soc.* **2003**, *125*, 15490−15498.
(6) Moore, M. H.; Donn, B.; Hudson, R. L. *Icarus* **1988**, *74*, 399−412.
(7) Borden, W. T.; Davidson, E. R. *J. Am. Chem. Soc.* **1977**, *99*, 4587−4594.
(8) Lenington, M. J.; Wenthold, P. G. *J. Phys. Chem. A* **2010**, *114*, 1334−1337.
(9) Odell, B. G.; Hoffman, R.; Imamura, A. *J. Chem. Soc. B* **1970**.
(10) Berson, J. A. In *Magnetic Properties of Organic Materials*; Lahti, P. M., Ed.; Marcel Dekker, Inc.: New York, 1999.
(11) Berson, J. A. *Acc. Chem. Res.* **1997**, *30*, 238−244.
(12) Matsumoto, T.; Ishida, T.; Koga, N.; Iwamura, H. *J. Am. Chem. Soc.* **1992**, *114*, 9952−9959.
(13) Lin, W.; Wilson, S. R.; Girolami, G. S. *Organometallics* **1997**, *16*, 2356−2361.
(14) Ikeda, H.; Tanaka, F.; Akiyama, K.; Tero-Kubota, S.; Miyashi, T. *J. Am. Chem. Soc.* **2003**, *126*, 414−415.
(15) Dowd, P.; Chang, W.; Paik, Y. H. *J. Am. Chem. Soc.* **1987**, *109*, 5284−5285.
(16) Bryan, C. D.; Cordes, A. W.; Goddard, J. D.; Haddon, R. C.; Hicks, R. G.; MacKinnon, C. D.; Mawhinney, R. C.; Oakley, R. T.; Palstra, T. T. M.; Perel, A. S. *J. Am. Chem. Soc.* **1996**, *118*, 330−338.
(17) Longuet-Higgins, H. C. *J. Chem. Phys.* **1950**, *18*, 265−274.
(18) Dowd, P.; Chang, W.; Paik, Y. H. *J. Am. Chem. Soc.* **1986**, *108*, 7417−7419.
(19) Clifford, E. P.; Wenthold, P. G.; Lineberger, W. C.; Ellison, G. B.; Wang, C. X.; Grabowski, J. J.; Vila, F.; Jordan, K. D. *J. Chem. Soc., Perkin Trans. 2* **1998**, 1015−1022.
(20) Bush, L. C.; Heath, R. B.; Feng, X. W.; Wang, P. A.; Maksimovic, L.; Song, A. I.; Chung, W.-S.; Berinstain, A. B.; Scaiano, J. C.; Berson, J. A. *J. Am. Chem. Soc.* **1997**, *119*, 1406−1415.
(21) Bush, L. C.; Maksimovic, L.; Feng, X. W.; Lu, H. S. M.; Berson, J. A. *J. Am. Chem. Soc.* **1997**, *119*, 1416−1427.
(22) Du, P.; Borden, W. T. *J. Am. Chem. Soc.* **1987**, *109*, 930−931.
(23) Nachtigall, P.; Jordan, K. D. *J. Am. Chem. Soc.* **1993**, *115*, 270−271.

(24) Nachtigall, P.; Jordan, K. D. *J. Am. Chem. Soc.* **1992**, *114*, 4743−4747.
(25) Rodríguez, E.; Reguero, M.; Caballol, R. *J. Phys. Chem. A* **2000**, *104*, 6253−6258.
(26) Filatov, M.; Shaik, S. *J. Phys. Chem. A* **1999**, *103*, 8885−8889.
(27) Pittner, J.; Nachtigall, P.; Čársky, P. *J. Phys. Chem. A* **2001**, *105*, 1354−1356.
(28) Bhaskaran-Nair, K.; Demel, O.; Šmydke, J.; Pittner, J. *J. Chem. Phys.* **2011**, *134*, 154106.
(29) Chattopadhyay, S.; Chaudhuri, R. K.; Mahapatra, U. S. *ChemPhysChem* **2011**, *12*, 2791−2797.
(30) Jastrow, R. *Phys. Rev.* **1955**, *98*, 1479−1484.
(31) McMillan, W. L. *Phys. Rev.* **1965**, *138*, 442−451.
(32) Ceperley, D.; Chester, G. V.; Kalos, M. H. *Phys. Rev. B* **1977**, *16*, 3081−3099.
(33) Anderson, J. B. *J. Chem. Phys.* **1980**, *73*, 3897−3899.
(34) Alfè, D.; Gillan, M. J. *J. Phys.: Condens. Matter* **2004**, *16*, L305−L311.
(35) Foulkes, W. M. C.; Mitas, L.; Needs, R. J.; Rajagopal, G. *Rev. Mod. Phys.* **2001**, *73*, 33−83.
(36) Anderson, J. B. *J. Chem. Phys.* **1975**, *63*, 1499−1503.
(37) Anderson, J. B. *J. Chem. Phys.* **1976**, *65*, 4121−4127.
(38) Manten, S.; Luchow, A. *J. Chem. Phys.* **2001**, *115*, 5362−5366.
(39) Roothaan, C. C. J. *Rev. Mod. Phys.* **1951**, *23*, 69−89.
(40) Møller, C.; Plesset, M. S. *Phys. Rev.* **1934**, *46*, 618−622.
(41) G. D., P., III; Bartlett, R. J. *J. Chem. Phys.* **1982**, *76*, 1910−1918.
(42) Scuseria, G. E.; Janssen, C. L.; Schaefer, H. F. *J. Chem. Phys.* **1988**, *89*, 7382−7387.
(43) McWeeny, R.; Diercksen, G. *J. Chem. Phys.* **1968**, *49*, 4852−4856.
(44) Knowles, P. J.; Andrews, J. S.; Amos, R. D.; Handy, N. C.; Pople, J. A. *Chem. Phys. Lett.* **1991**, *186*, 130−136.
(45) Watts, J. D.; Gauss, J.; Bartlett, R. J. *J. Chem. Phys.* **1993**, *98*, 8718−8733.
(46) Kohn, W.; Sham, L. J. *Phys. Rev.* **1965**, *140*, 1133−1138.
(47) Perdew, J. P.; Burke, K.; Ernzerhof, M. *Phys. Rev. Lett.* **1996**, *77*, 3865−3868.
(48) Adamo, C.; Barone, V. *J. Chem. Phys.* **1999**, *110*, 6158−6170.
(49) Dunning, T. H. *J. Chem. Phys.* **1989**, *90*, 1007−1023.
(50) Frisch, M. J.; Trucks, G. W.; Schlegel, H. B.; Scuseria, G. E.; Robb, M. A.; Cheeseman, J. R.; Scalmani, G.; Barone, V.; Mennucci, B.; Petersson, G. A.; Nakatsuji, H.; Caricato, M.; Li, X.; Hratchian, H. P.; Izmaylov, A. F.; Bloino, J.; Zheng, G.; Sonnenberg, J. L.; Hada, M.; Ehara, M.; Toyota, K.; Fukuda, R.; Hasegawa, J.; Ishida, M.; Nakajima, T.; Honda, Y.; Kitao, O.; Nakai, H.; Vreven, T.; Montgomery, J. A., Jr.; Peralta, J. E.; Ogliaro, F.; Bearpark, M.; Heyd, J. J.; Brothers, E.; Kudin, K. N.; Staroverov, V. N.; Kobayashi, R.; Normand, J.; Raghavachari, K.; Rendell, A.; Burant, J. C.; Iyengar, S. S.; Tomasi, J.; Cossi, M.; Rega, N.; Millam, J. M.; Klene, M.; Knox, J. E.; Cross, J. B.; Bakken, V.; Adamo, C.; Jaramillo, J.; Gomperts, R.; Stratmann, R. E.; Yazyev, O.; Austin, A. J.; Cammi, R.; Pomelli, C.; Ochterski, J. W.; Martin, R. L.; Morokuma, K.; Zakrzewski, V. G.; Voth, G. A.; Salvador, P.; Dannenberg, J. J.; Dapprich, S.; Daniels, A. D.; Farkas, O.; Foresman, J. B.; Ortiz, J. V.; Cioslowski, J.; Fox, D. J. *Gaussian 09*, revision A.1; Gaussian, Inc.: Pittsburgh, PA, 2009.
(51) Hegarty, D.; Robb, M. A. *Mol. Phys.* **1979**, *38*, 1795−1812.
(52) Eade, R. H. A.; Robb, M. A. *Chem. Phys. Lett.* **1981**, *83*, 362−368.
(53) Yamamoto, N.; Vreven, T.; Robb, M. A.; Frisch, M. J.; Schlegel, H. B. *Chem. Phys. Lett.* **1996**, *250*, 373−378.
(54) Xu, J.; Deible, M. J.; Peterson, K. A.; Jordan, K. D. *J. Chem. Theory Comput.* **2013**, *9*, 2170−2178.
(55) Trail, J. R.; Needs, R. J. *J. Chem. Phys.* **2005**, *122*, 174109.
(56) Trail, J. R.; Needs, R. J. *J. Chem. Phys.* **2005**, *122*, 014112.
(57) Needs, R. J.; Towler, M. D.; Drummond, N. D.; Lopez Rios, P. *J. Phys.: Condens. Matter* **2010**, *22*, 023201.
(58) Drummond, N. D.; Towler, M. D.; Needs, R. J. *Phys. Rev. B* **2004**, *70*, 235119.
(59) Umrigar, C. J.; Toulouse, J.; Filippi, C.; Hennig, R. G. *Phys. Rev. Lett.* **2007**, *98*, 110201.
(60) Umrigar, C. J.; Nightingale, M. P.; Runge, K. J. *J. Chem. Phys.* **1993**, *99*, 2865−2890.
(61) Casula, M. *Phys. Rev. B* **2006**, *74*, 161102(R).
(62) Flyvbjerg, H.; Petersen, H. G. *J. Chem. Phys.* **1989**, *91*, 461−466.
(63) Andersson, K.; Malmqvist, P.-Å.; Roos, B. O. *J. Chem. Phys.* **1992**, *96*, 1218−1226.
(64) Celani, P.; Werner, H.-J. *J. Chem. Phys.* **2000**, *112*, 5546−5557.
(65) Werner, H.-J.; Knowles, P. J.; Knizia, G.; Manby, F. R.; Schutz, M.; Celani, P.; Korona, T.; Lindh, R.; Mitrushenkov, A.; Rauhut, G.; Shamasundar, K. R.; Adler, T. B.; Amos, R. D.; Bernhardsson, A.; Berning, A.; Cooper, D. L.; Deegan, M. J. O.; Dobbyn, A. J.; Eckert, F.; Goll, E.; Hampel, C.; Hesselmann, A.; Hetzer, G.; Hrenar, T.; Jansen, G.; Koppl, C.; Liu, Y.; Lloyd, A. W.; Mata, R. A.; May, A. J.; McNicholas, S. J.; Meyer, W.; Mura, M. E.; Nicklass, A.; O'Neill, D. P.; Palmieri, P.; Peng, D.; Pfluger, K.; Pitzer, R.; Reiher, M.; Shiozaki, T.; Stoll, H.; Stone, A. J.; Tarroni, R.; Thorsteinsson, T.; Wang, M. *MOLPRO, version 2012.1, a package of ab initio programs*; 2012.
(66) Lindh, R.; Ryu, U.; Liu, B. *J. Chem. Phys.* **1991**, *95*, 5889−5897.
(67) Raghavachari, K.; Anderson, J. B. *J. Phys. Chem.* **1996**, *100*, 12960−12973.
(68) Bressanini, D. *Phys. Rev. B* **2012**, *86*, 115120.
(69) Gritsenko, O. V.; Schipper, P. R. T.; Baerends, E. J. *J. Chem. Phys.* **1997**, *107*, 5007−5015.
(70) Pulay, P. *Int. J. Quantum Chem.* **2011**, *111*, 3273−3279.